Drug Development and Industrial Pharmacy, 28(2), 165–175 (2002)

RESEARCH PAPER

Acetylation Enhances the Tabletting Properties of Starch

Pasi Raatikainen,[1,*] Ossi Korhonen,[1]
Soili Peltonen,[2] and Petteri Paronen[1]

[1]*University of Kuopio, Department of Pharmaceutics, P.O. Box 1627, FIN-70211 Kuopio, Finland*
[2]*VTT Chemical Technology, Materials Technology, P.O. Box 21, FIN-05201 Rajamäki, Finland*

ABSTRACT

*The aim of this study was the evaluation of starch acetate (SA) powders used as tablet excipients. Deformation during powder volume reduction, strain-rate sensitivity, intrinsic elasticity of the materials, and tensile strength of the tablets were examined. Results showed that SA with the lowest degree of substitution (*ds*) still possessed characteristics of native starch granules. Due to dissolution in synthesis, the properties of higher* ds *SAs depended on precipitation and drying processes. The acetate moiety, perhaps in combination with existing hydroxyl groups, was a very effective bond-forming substituent. The formation of strong molecular bonds increased, leading to a very firm and intact tablet structure. Small changes existed in compression-induced deformation due to acetylation. Some fragmentation was induced due to the slightly harder and more irregular shape of high-substituted SA particles. The plastic flow under compression was enhanced. Acetylated material was slightly less sensitive to fast elastic recovery in-die, but somewhat more elastic out-of-die. In spite of their superior bonding, SAs under compression behaved similarly to native starches. It was concluded that deformation properties were more the consequence of the molecular chain structure properties of the starch polymer than the effect of the acetate moiety itself. In contrast, the opposite seemed to be the case with the extensive improvement in bond-forming properties.*

Key Words: *Elasticity; Mechanical strength; Plastic flow; Starch acetates; Strain-rate sensitivity; Tabletting*

*Corresponding author. Fax: +358-17-162-252; E-mail: praatika@messi.uku.fi

INTRODUCTION

A new group of pharmaceutical excipients has recently been described (1–3). This group is based on acetylation of native starch, resulting in the formation of starch acetates (SAs). During the treatment, native starch is mixed with acetic acid anhydride in the presence of a catalyst producing SA, i.e., starch polymer, where the hydroxylic moieties of glucose monomers are partially substituted by acetate groups. Depending on the reaction conditions, the product is a starch with a certain acetate degree of substitution (*ds*). The known particle and powder properties, i.e., size, shape, and flowability, depend on the precipitation and drying phases of SA manufacture (1). The functionality of SAs in tablet formulation depends strongly on the acetate moiety content (2,3). A low degree of substitution emphasizes disintegrant, filler, and dry-binder functionality. Starch with acetate *ds* about or above 2.0 forms, under compression, block-like intact structures suitable for controlled-release applications. SAs have excellent bond-forming ability (1). The reason for the enhanced bonding compared with native starch is still unclear. Until now a detailed evaluation of the deformation properties of SAs has not been reported.

A series of acetylated starches provides quite an unusual opportunity to examine the roles of the starch polymer backbone, as well as the moiety attached to the glucose units, acetate in the present case, in the bonding and deformation of particulate starches under compression. The deformation properties of differently substituted SAs were evaluated in parallel with the three commercially-available and widely-characterized direct compression excipients.

MATERIALS AND METHODS

Materials

The SAs supplied by manufacturer VTT, Chemical Technology (Rajamäki, Finland) had a *ds* of 0.34, 1.19, 2.1, and 2.9. The materials were synthetized by allowing native barley starch to react with varying amounts of acetic acid anhydride in the presence of a 50% sodium hydroxide solution catalyst (2). After the reaction phase, the mixture was cooled and the barley SA was precipitated from the water with vigorous mixing. The precipitate was filtered and washed thoroughly with water, then dried using the fluidizied bed method (Anhydro fluid bed No. 38, APV Anhydro AS, Denmark; fluid bed 140°C, endpoint moisture less than 5%). The materials in the comparison were microcrystalline cellulose (MCC) (Avicel PH 101®, FMC, Philadelphia, PA), dicalcium phosphate dihydrate (DCP) (Emcompress®, Penwest Pharmaceuticals, Patterson, NY), and pregelatinized starch (PS) (Starch 1500®, Colorcon, West Point, PA). Commercial excipients were used as supplied, and sieve fractions 59–297 μm of the SAs. All the particulate materials were stored at room temperature (20°C) in a closed container under 45% relative humidity (RH) at least two weeks before the compaction of samples.

Methods

Particle Properties

The apparent particle density of materials was measured by means of an air comparison pycnometer (Quantachrome Multipycnometer, Syosset, NY,USA) using helium as an inert measurement gas. The water content was determined using a Karl Fischer titrator (Mettler DL 35, Greifensee, Switzerland). Four repeated measurements were performed with the above-mentioned tests. The mean particle size of materials was determined by measuring the dimensions of 400 particles from scanning electron micrographs (Jeol JSM-35, Tokyo, Japan), and the results were described as Martin's diameter. The ratio between equivalent diameters of the sphere having the same area, and the sphere having the same perimeter, was referred to as the sphericity of particles. A larger value indicates that particles are becoming more regular and unity represents totally spherical particles.

Tablet Compaction

Quantities of particulate materials for tablets were individually weighed into the die according to the apparent particle density of materials. The weight of the powder was adjusted to produce tablets with a theoretical zero porosity thickness at 1.5 mm. Compaction of tablets was performed using a compaction simulator (Puuman Ltd., Kuopio, Finland) equipped with flat-faced punches (Ø 10 mm). Four repeated experiments were performed. The die was not lubricated, except for DCP, in

which case, due to extensive sticking, 2% magnesium stearate (Ph. Eur.) in acetone was applied to the die walls with a paintbrush and allowed to dry. A single-sided sawtooth compaction profile was used, i.e., the strain rate of the upper punch was the same during compression and decompression phases (lower punch stationary), and the deformation of punches was taken into account when the strain data were calculated. Compression speeds were 3 and 300 mm/sec. The tablets were weighed after compaction. The tablets were then stored for 24 hr in a closed container under 45% RH at 20°C room temperature. The dimensions of the tablets were measured using a micrometer. The breaking strength of the tablets was measured using a universal tester (CT-5, Engineering Systems, Nottingham, UK) with cross-head load rate of 1 mm/sec. The results were calculated and described as tensile strength values (4). The tablet surfaces were evaluated from scanning electron micrographs (Jeol JSM-35, Japan).

DSC Measurement

A differential scanning calorimeter (DSC) (Perkin-Elmer DSC-7, Perkin-Elmer Co., Norwalk, Connecticut, USA) was used in the determination of the glass transition temperatures (T_g) of the compressed tablets. Carefully ground tablet samples (4–6 mg) were closed in perforated 50-μL aluminum pans. The following program was followed: heating from 20 to 200°C (20°C/min); cooling to 100°C (20°C/min); heating to 200°C (10°C/min). The glass transition temperature was determined as the mean of three parallel scans. This method was used by Korhonen et al. (1) with the SA powders also used in this study. Thus the results are directly comparable.

Evaluation of Compaction Data

The evaluation of deformation was made by means of the Heckel equation (5,6):

$$\ln\left[\frac{1}{1-D}\right] = kP + A \tag{1}$$

which relates the relative density D (ratio of apparent tablet and particle densities) to the applied pressure P. The reciprocal of the slope (k) of the Heckel plot is referred to as the yield pressure (K). For further calculations the most linear portion of the plot was chosen as the range of pressure which gave the best least-squares fit to the linear model. The F-ratio between the model and the residual estimated the fit. The linear portion coincided with successive data (highest F-ratio). The constant A in the Heckel equation is related to the initial packing and particle rearrangement phases, before deformation and bonding of particles (5,6). The relative densities were related by:

$$D_A = D_0 + D_B \tag{2}$$

where D_0 describes the effect of initial packing (achieved in this study when a measurable minimum force of 10 N was reached), D_B represents the particle rearrangement phase, and D_A includes both the initial packing and particle rearrangement phases.

Yield pressures were calculated by both the tablet-in-die and the ejected-tablet methods (7). In the tablet-in-die method, yield pressures were calculated during both compression and decompression phases. Yield pressure during compression (K_d) is a parameter describing the total deformation (both plastic and elastic). Yield pressure during decompression (K_{ef}) represents the fast elastic deformation of the compact (8). In the ejected-tablet method, the relative density was calculated using the dimensions of the compact measured 24 hr after the compression. By subtracting the Heckel plot slopes of tablet-in-die from the slopes of the ejected tablets and calculating the reciprocal, the yield pressure (K_{et}) describing the total elastic tendency of the material is determined.

The sensitivity of materials toward time-dependent deformation during compression, or the strain-rate sensitivity (SRS), was evaluated by (9):

$$1 - \frac{K_{d(3)}}{K_{d(300)}} \times 100(\%) \tag{3}$$

where $K_{d(3)}$ and $K_{d(300)}$ are the yield pressures at compaction speeds of 3 and 300 mm/sec, respectively.

Beam-Bending Measurements

The intrinsic elasticity of the materials (Young's modulus) was evaluated by the three-point bending method. Rectangular beams were compressed using a manual hydraulic press (Pye Unicam, Carver Press, Wabash, USA) and varying the weight of the powder in the die. To prevent excessive sticking with DCP, the die was lubricated with 2% magne-

sium stearate (Ph. Eur.) in acetone, applied to the die walls with a paintbrush and allowed to dry. At least eight beams with a cross-section of $1.0 \times 6.0 \times 30.0\,mm^3$ (± 0.1) were compressed. The dwell time was 10 sec. Porosity ranges were 12–42%, 11–47%, 6–56%, 6–58%, 5–49%, and 14–29% for SAs with *ds* 0.34, 1.19, 2.1, 2.9, MCC, and DCP beams, respectively. PS could not form measurable beams. Compressed beams were stored for 24 hr in a closed container under 45% RH at 20°C room temperature before taking the three-point bending measurement with a universal tester (CT-5, cross-head load rate of 1 mm/sec, Engineering Systems, UK). The span distance was adjusted to 20 mm. The elasticity (E) of a sample was calculated from the linear part of the stress/-strain data:

$$E = \frac{Fl^3}{4D_m bh^3} \tag{4}$$

where F is the load, l is the distance between the beam supports, D_m is the displacement at the middle point of the beam, h is the thickness, and b the width of the beam. The values were then extrapolated to zero porosity using the exponential (10):

$$E = E_0 \exp(-cP) \tag{5}$$

where E_0 is Young's modulus at zero porosity, c is constant, and P is porosity.

RESULTS

Particle Characteristics

Korhonen et al. (1) evaluated the same particulate SAs with x-ray diffractometry and reported that the acetylation process produced a more amorphous form of SAs, with *ds* from 1.19 to 2.9, compared with the minor ordered crystalline regions with *ds* 0.34. While the glass transition point could be expected to change due to acetylation, it was reported to be unchanged.

Figure 1 shows that the particles of SA with *ds* 0.34 were rather similar to barley native starch granulates, i.e., very small spherical particles and their aggregates. The typical particle characteristics of starch granulates disappeared when *ds* was above 0.34. The mean particle size of the SA with *ds* 1.19 was the smallest of the SAs, when the *ds* increased above that value, particle size again increased (Table 1). Regularity in particle shape diminished clearly (Fig. 1), as also noticed from the shape factor (Table 1). A clear decrease in water content was noticed as *ds* was increased.

Properties of Tablets

Glass transition temperatures of the samples ground from compressed SA tablets were unchanged compared with corresponding SA powders; T_g values varied from 156 to 166°C. No correlation existed with the *ds*. Weighing the samples before and after DSC measurements validated the method. The weight loss corresponded accurately with the dehydration, indicating that no chemical degradation had occurred during thermal measurements.

Figure 2 shows the tensile strength values of the tablets. Increasing the compaction force improved the tensile strength of the tablets prepared from all materials. No capping of tablets was noticed. Increasing the compression speed decreased the strength of the tablets prepared from all materials, with the exception of DCP. The latter is generally known to deform mainly by fragmentation. Time dependence is typical for plastic flow materials.

The tensile strength of the SA *ds* 0.34 tablets was somewhat better than that of the DCP tablets. The tensile strengths of the SA *ds* 1.19–2.9 and MCC tablets were similar. However, the tensile strength of the SA *ds* 1.19–2.9 tablets with higher compaction pressures did not increase to the same levels as that of the MCC tablets. The difference was even clearer when comparing the changes in tablet porosities (Fig. 3). In the compression pressure range from 200 to 250 MPa the porosity changed only 0.020–0.029%/MPa for SA *ds* 1.19–2.9, compared with 0.045%/MPa for MCC. Thus, both the breaking strength and tablet porosity of SA tablets seemed to approach a constant plateau level, where the addition of compression pressure has practically no effect on tablet properties.

Packing During Compression

The relative density values presented in Fig. 4 describe the densification state reached with the cumulative processes of initial packing [10 N detected force (D_0)], rearrangement of particles (D_B), and 150 MPa compression in the die (D_{150}). An increase in the *ds* tended to make the SA

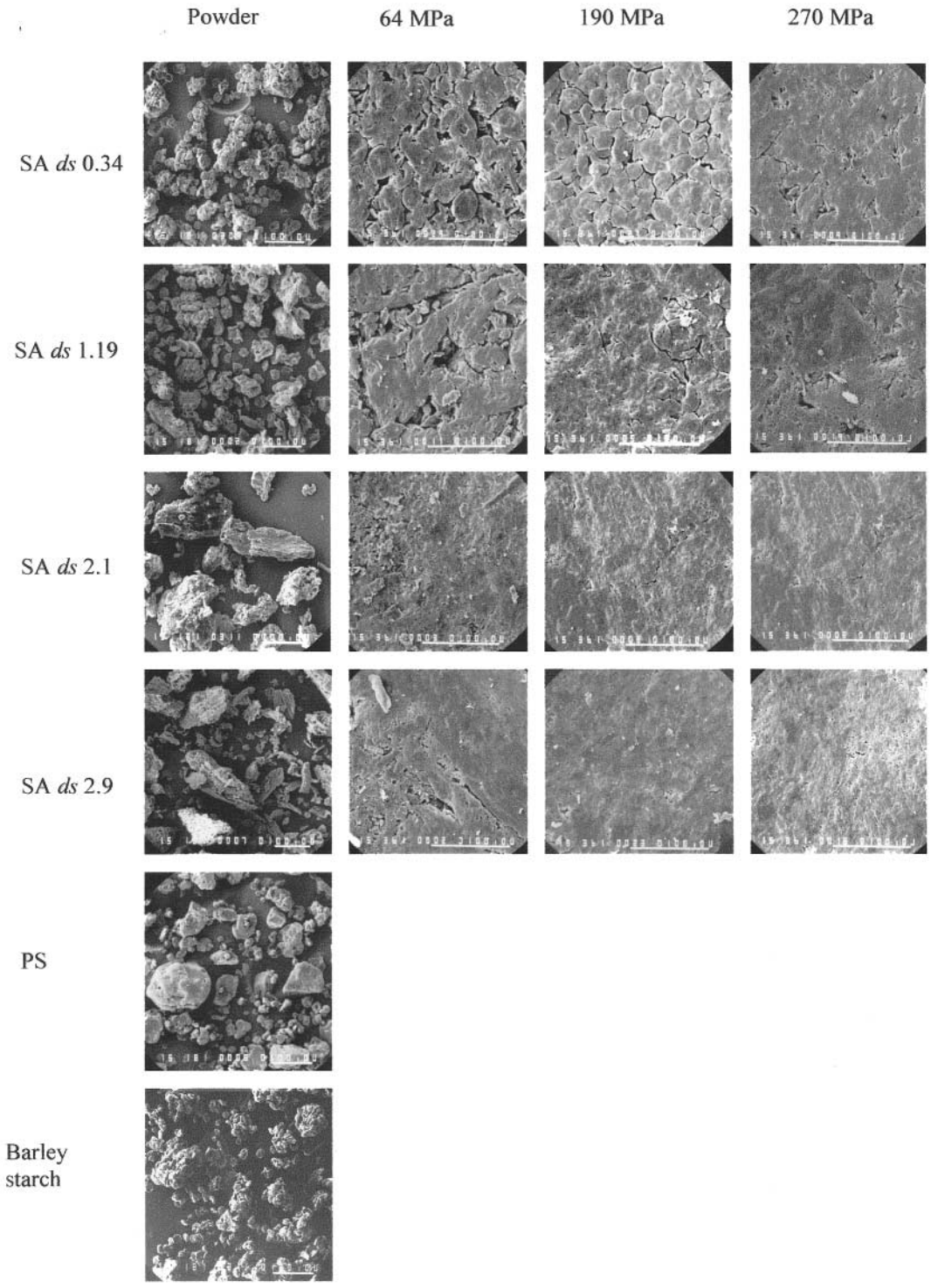

Figure 1. Scanning electron micrographs of powder particles and tablets compressed at a speed of 300 mm/sec to the pressure of 64, 190 and 270 MPa. Bar is 100 mm.

Table 1

Powder and Particle Characteristics of Materials

Material	Particle Density (g/cm^3)	Martin's Diameter (μm)	Water Content (%)	Sphericity
SA *ds* 0.34	1.515	49 ± 47	7.5 ± 0.01	0.892
SA *ds* 1.19	1.461	32 ± 21	5.2 ± 0.04	0.883
SA *ds* 2.1	1.390	55 ± 38	2.4 ± 0.02	0.845
SA *ds* 2.9	1.367	69 ± 55	1.5 ± 0.02	0.821
MCC	1.656	30 ± 21	5.0 ± 0.12	0.714
PS	1.558	30 ± 27	8.0 ± 1.43	0.853
DCP	2.301	163 ± 17	0.7 ± 0.19	0.871

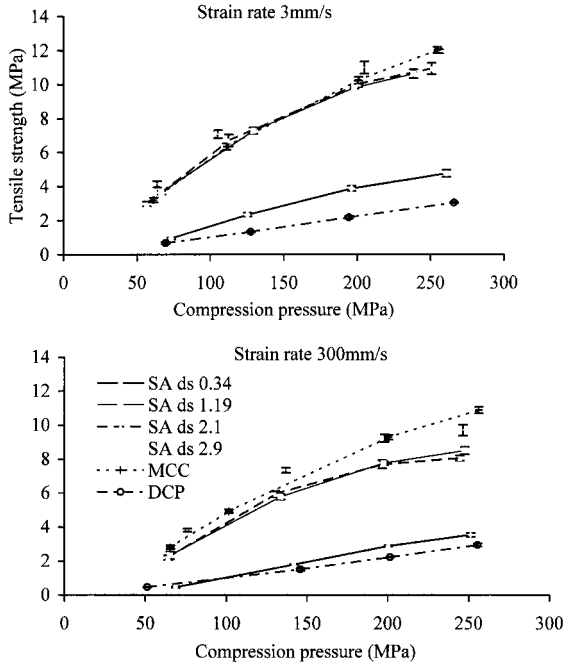

Figure 2. Tensile strength values of tablets.

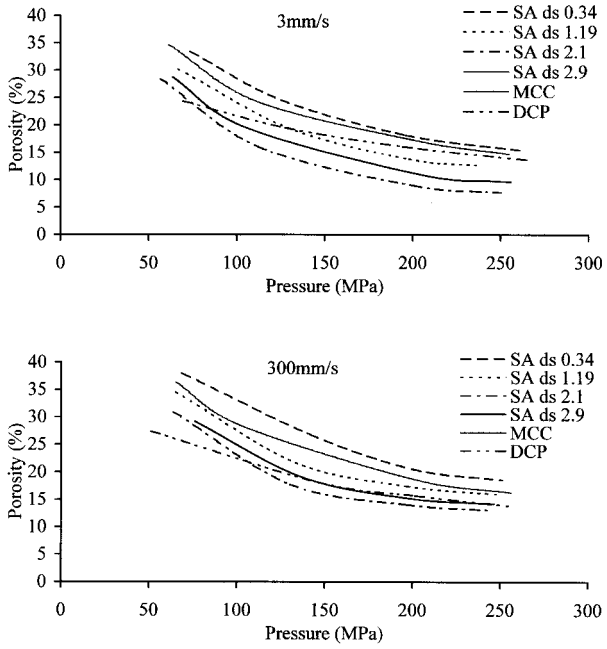

Figure 3. Porosity change of tablets.

particles more irregular (Table 1) and the powder bed was less dense at the initial packing phase of tablet compression. Particle size also increased, which could affect the density. The D_0 values of the SAs were nearest to the D_0 level of MCC, which also consists of rather small and irregular particles. When the compression speed was increased, the densification through initial packing at the very beginning of tablet compression became more difficult for all the materials tested (Fig. 4). This has also been shown for several other pharmaceutical materials (11,12).

The D_B values, describing particle rearrangement, for the SAs were relatively close to those of MCC (Fig. 4). Due to the very dense initial packing structure (perhaps close to the most dense possible) of PS compact formed under low compression speed, the rearrangement had only a minor densification effect. DCP underwent more rearrangement than any of the other materials. This was most probably induced by partial particle fragmentation of the DCP particles at the very start of tablet compression. In parallel with the results on D_0, an increase in the compaction speed

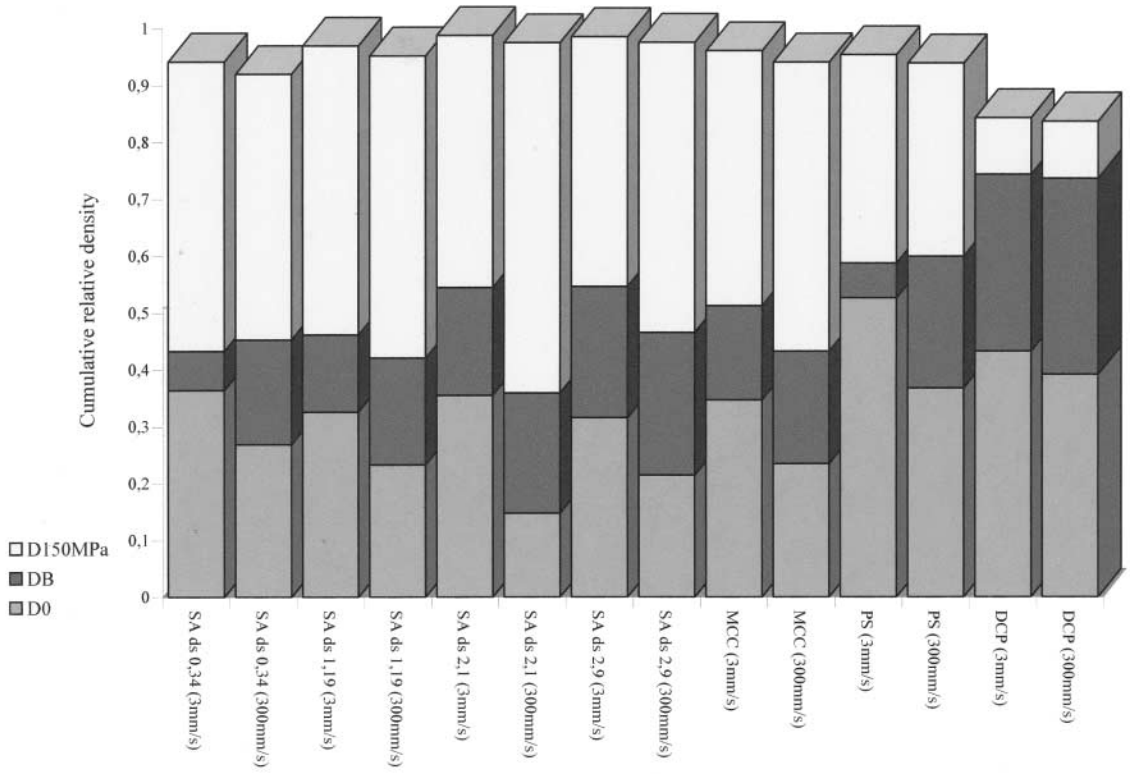

Figure 4. Relative density values of materials (cumulative progress).

decreased the obtained D_A densification for all the materials except SA *ds* 0.34 and PS. Similar behavior has been demonstrated for several other very soft pharmaceutical materials (11,12). The increased velocity leads to localized high stresses and plastic flow of very soft particles (the isthmus effect) when particles are impacted against each other. This effect was not present with the SAs having *ds* over 1. According to the Heckel theory, the densification through deformation (i.e., elastic deformation, plastic flow, fragmentation) begins when the densification process exceeds the relative densification stage illustrated by the D_A value. Our results, however, demonstrated exceptions with the fragmenting DCP, very soft SA *ds* 0.34, and PS.

The relative densification of the compacts under a pressure of 150 MPa (D_{150}) shows that all the materials achieved effective compact densification except DCP, because of its particle fragmentation and sticking in the die.

Deformation During Volume Reduction

The general shape of in-die upward Heckel plots (Fig. 5) was almost identical for all the SAs. There was a very short initial curvature related to extensive plastic deformation and softness of material (13). However, a minor difference between SA *ds* 0.34, PS, and higher *ds* SAs could be noticed. Higher *ds* SAs showed a slightly more extensive initial curvature, indicating that the higher *ds* SA particles somewhat lacked the typical softness of starch granulates. Deformation following the rearrangement was probably partially through fragmentation of corners and asperities of more irregular high *ds* SA particles. This is also supported by the scanning electron micrographs (Fig. 1). Tablets in the figures were compressed at a speed of 300 mm/sec. With SA *ds* 0.34 the contours of primary starch particles could still be recognized even at the highest compaction pressure, but disappearance of the contours was noticed at both

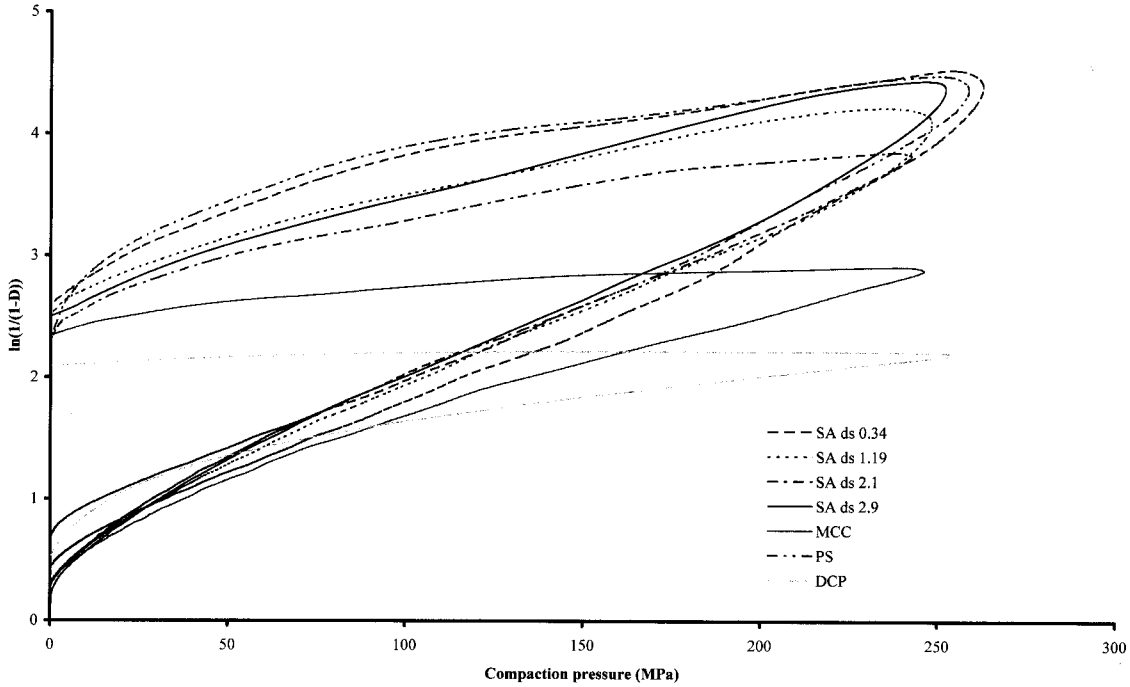

Figure 5. In-die Heckel plots of materials.

compaction speeds at a compaction pressure of 190 MPa (±6) with SA *ds* 1.19, and at the lowest compaction pressure [of 64 MPa (±4)] with SAs *ds* 2.1 and 2.9. Above those compaction forces the micrographs of the tablets looked the same, i.e., like very solid, smooth-surfaced, block-like tablets. The disappearance of the contours has been pointed out to reflect the deformation of primary particles by fragmentation (14). Other parameters measured here, however, indicated only minor initial fragmentation but extensive plastic deformation of all the SAs. Yield pressures decreased slightly as the *ds* increased from 0.34 to 2.1 (K_d, Table 2). The values of *ds* 2.1 and 2.9 were practically the same. Thus, although the particles of higher *ds* SAs were characterized as somewhat less soft than typical starch particles, their deformation under compression load was enhanced as the *ds* increased above 1. Compared with the other materials, the yield pressures of PS were similar to those of SA *ds* 0.34, whereas MCC was at the level between SAs *ds* 0.34 and 1.19. The values of DCP were clearly higher than the values of all the other materials, which was to be expected for a material deforming mainly by fragmentation (15).

Strain-Rate Sensitivity

The yield pressure values of total deformation (K_d) were used in the strain-rate sensitivity calculations (SRS values, Table 2). All the materials excluding DCP showed dependency on the changing compaction speed, indicating that the deformation was time-dependent. The rank order of the SRS values of PS, MCC, and DCP corresponds to the literature values (9). The results showed that SAs *ds* 0.34 and 1.19 were at the level of PS, and SAs *ds* 2.1 and 2.9 were at the level of MCC. Interestingly, SAs were less sensitive toward increasing strain rate as the *ds* increased. This confirms that the deformation of SAs with *ds* above 0.34 was at least partially through time-independent fragmentation. However, the nominal SRS differences between the SAs indicate fragmentation is a minor portion of deformation.

Table 2

Yield Pressures (MPa) from the Heckel Plots and the Strain-Rate Sensitivity (SRS) of Materials

	K_d			K_{ef}		K_{et}	
Material	3 mm/sec	300 mm/sec	SRS (%)	3 mm/sec	300 mm/sec	3 mm/sec	300 mm/sec
SA *ds* 0.34	66 ± 7	78 ± 2	15.4	132 ± 38	120 ± 43	91	114
SA *ds* 1.19	52 ± 6	60 ± 2	13.3	135 ± 25	103 ± 29	71	80
SA *ds* 2.1	41 ± 3	46 ± 3	10.9	179 ± 12	170 ± 9	57	59
SA *ds* 2.9	43 ± 3	48 ± 1	10.4	191 ± 20	182 ± 25	57	60
MCC	59 ± 2	66 ± 2	10.6	327 ± 22	237 ± 19	79	91
PS	68 ± 2	79 ± 4	13.9	244 ± 58	181 ± 41	[a]	[a]
DCP	305 ± 10	312 ± 10	2.2	3589 ± 756	2720 ± 420	3087	−6417

[a]PS could not form measurable tablets.

Elasticity of Tablets

Yield pressure values describing fast and total elastic deformation, gained by the tablet-in-die and combination methods (K_{ef} and K_{et}; Table 2, respectively) highlighted the dependency of elastic recovery on the *ds* of the SA compacts. Generally, K_{ef} values indicated that all the SAs were prone to recover already in-die. The values were lower than those of MCC and DCP, and even lower than those of PS, which is reported to have a major fast elastic property (16). Generally, according to the K_{et} values, all the compacts except those of DCP were prone to extensive recovery. For all the materials, the increase in compaction speed increased the fast elastic tendency but decreased the tendency toward total elastic recovery of the compacts. This compaction speed effect might reflect the enhanced interaction of particles during volume reduction, i.e., slow speed compression created stronger interactions through prolonged deformation time and was reflected by less elastic recovery of the compact in-die.

For SA tablets, increasing acetate moiety content seemed to change the elastic tendency slightly from fast 'in-die'' toward slower ''ejected-tablet'' recovery. The lowest K_{ef} values were with SAs *ds* 0.34 and 1.19, and the lowest K_{et} values were with SAs *ds* 2.1 and 2.9.

Young's Modulus Values

According to the Young's modulus values, the SA beams were more elastic than those of MCC or DCP (E_0 values, Table 3). The Young's modulus values for DCP and MCC are in agreement with previously published data (17–21). Church and Kennerley (17) have also published beam-bending values for PS, and the Young's modulus reported as 1.35 GPa (at relative density of 0.81), which indicates the high elasticity of starches and is in correlation with SAs, considering the values of SAs at approximately the same (20%) porosity. With respect to the SAs, an increase in *ds* slightly decreased the intrinsic elasticity, however, the difference between the lowest and highest SA *ds* was small.

Table 3

Young's Modulus Values (GPa) of Materials

Material	E_0	c	r^2
SA *ds* 0.34	2.61	0.0227	0.989
SA *ds* 1.19	2.91	0.0257	0.995
SA *ds* 2.1	2.96	0.0441	0.998
SA *ds* 2.9	3.65	0.0481	0.996
MCC	6.60	0.0503	0.993
DCP	32.84	0.0888	0.977

DISCUSSION

During SA synthesis the material partially (below about *ds* 0.8) or totally (over *ds* 0.8) dissolves. Thus, the low-substituted SA properties are similar to the native barley starch granules used as starting material

in the synthesis. According to the literature (22,23) the orientation of the starch molecular chains is perpendicular to the surface of the starch granule. Therefore, the number of molecular chains terminating at the surface of the granule is very high. The surface is resistant to chemical or physical attack. Therefore, the low-substituted SAs may contain a higher amount of acetate moieties on the surface of the granules than inside the granule structure. It is also reasonable to suppose that the molecular orientation of native starch components—amylose and amylopectin—remains unchanged in undissolved material, despite the acetylation of the surface layer of the starch granule. The total collapse of the granule structure does occur with stronger (or longer) treatment with acetic anhydride in a base-catalyzed esterification process. This produces the high *ds* SA particles that demonstrate no starch granule similarities. Korhonen et al. (1) showed that the particle and powder properties of the higher substituted SAs are dependent on the precipitation and drying phases of manufacture.

The water content of starch was dramatically decreased due to acetylation. Water is mainly nonspecifically bound to starch and no specific water-filled cavities exist. However, water is an important material supporting interchain hydrogen bonding in the starch material. Replacing the hydroxyl groups in the starch with acetate moieties decreased the hydrophilicity of the material. Although all the hydroxyl groups were replaced, possibilities still exist for hydrogen bonding. However, due to acetylation, the formation of strong molecular bonds, like van der Waal's forces, is increased several-fold. The activation of these forces requires very intimate contact of the molecular structures. According to the reported firm structure of SA tablets, the compression was able to induce favorable conditions for interchain bonding in SA material. As could be concluded from the results of low-substituted SA tablets, the acetate moiety, perhaps in combination with existing hydroxyl groups, seemed to be a very effective bond-forming substituent in starches. An increase in the *ds*, at least up to *ds* 2.1, made SA tablets even stronger.

CONCLUSIONS

There existed only small changes in compression-induced particles and compact deformation due to acetylation of starches. Most probably some fragmentation was induced due to the slightly harder and more irregular shape of high-substituted SA particles. On the other hand, the plastic flow under compression was slightly enhanced. Acetylation also modified the material to be slightly less sensitive to fast elastic recovery in-die, but also to be somewhat more time-dependently elastic after ejection from the die. Generally, the reported changes were small, and the SAs under compression behaved similarly to native starch materials. This is even more surprising when taking into account that in the *ds* 2.9 SA, the acetate component forms over 40% of the mass of the material. If the above discussion is valid, and the molecular chain configuration was not changed dramatically because of the acetylation, one can conclude that the deformation properties are more a consequence of the molecular chain structure properties of the starch polymer backbone than the effect of the acetate moiety itself. On the other hand, the opposite seemed to be the case in the situation with the extensive improvement in bond-forming properties.

REFERENCES

1. Korhonen, O.; Raatikainen, P.; Harjunen, P.; Nakari, J.; Suihko, E.; Peltonen, S.; Vidgren, M.; Paronen, P. Starch Acetates—Multifunctional Direct Compression Excipients. Pharm. Res., **2000**, *17*, 1138–1143.
2. Paronen, P.; Peltonen, S.; Urtti, A.; Nakari, J. SA Composition with Modifiable Properties, Method for Preparation and Usage Thereof. US Patent 5667803, 1997.
3. Raatikainen, P.; Paronen, P.; Peltonen, S.; Nakari, J.; Urtti, A. Starch Acetates: Multifunctional Excipients for Tabletting. In Proceedings of 16th Pharmaceutical Technology Conference, Solid Dosage Research Unit, Liverpool, UK, 1997; Rubinstein, M.H., Ed.; Vol. II, 192–193.
4. Fell, J.T.; Newton, J.M. Determination of Tablet Strength by the Diametral Compression Test. J. Pharm. Sci. **1970**, *59*, 688–691.
5. Heckel, R.W. Density Pressure Relationship in Powder Compaction. Trans. Metall. Soc. AIME **1961**, *221*, 671–675.
6. Heckel, R.W. An Analysis of Powder Compaction Phenomena. Trans. Metall. Soc. AIME **1961**, *221*, 1001–1008.
7. Paronen, P.; Juslin, M.J. Compressional Characteristics of Four Starches. J. Pharm. Pharmacol. **1983**, *35*, 627–635.

8. Duberg, M.; Nyström, C. Studies on Direct Compression of Tablets. XVII. Porosity–Pressure Curves for the Characterization of Volume Reduction Mechanisms in Powder Compression. Powder Technol. **1986**, *46*, 67–75.
9. Roberts, R.J.; Rowe, R.C. The Effect of Punch Velocity on the Compaction of a Variety of Materials. J. Pharm. Pharmacol. **1985**, *37*, 377–384.
10. Spriggs, R.M. Expression for Effect of Porosity on Elastic Modulus of Polycrystalline Refractory Materials, Particularly Aluminium Oxide. J. Am. Ceram. Soc. **1961**, *44*, 628–629.
11. Roberts, R.J.; Rowe, R.C. The Effect of the Relationship Between Punch Velocity and Particle Size on the Compaction Behaviour of Materials with Varying Deformation Mechanisms. J. Pharm. Pharmacol. **1986**, *38*, 567–571.
12. Muñoz-Ruiz, A.; Paronen, P. Time-Dependent Densification Behaviour of Cyclodextrins. J. Pharm. Pharmacol. **1996**, *48*, 790–797.
13. Doelker, E. Recent Advances in Tableting Science. Boll. Chim. Pharm. **1988**, *127*, 37–49.
14. Pesonen, T.; Paronen, P. Compressional Behaviour of an Agglomerated Cellulose Powder. Drug. Dev. Ind. Pharm. **1990**, *16*, 591–612.
15. Muñoz-Ruiz, A.; Payán Villar, T.; Muñoz Muñoz, N.; Monedero Perales, M.C.; Jiménez-Castellanos, M.R. Analysis of the Physical Characterization and the Tablettability of Calcium Phosphate Based Materials. Int. J. Pharm. **1994**, *110*, 37–45.
16. Paronen, P. Heckel Plots as Indicators of Elastic Properties of Pharmaceuticals. In Tableting Technology, Series in Pharmaceutical Technology; Rubinstein, M.H., Ed.; Ellis Horwood: Chichester, UK, 1987; 139–144.
17. Church, M.S.; Kennerley, J.W. An Evaluation of Four-Point Bending for the Mechanical Characterization of Compacted Pharmaceutical Materials. In Proceedings of 4th Pharmaceutical Technology Conference, Solid Dosage Research Unit, Liverpool, UK, 1984; Rubinstein, M.H., Ed.; Vol. I, 185–215.
18. Bassam, F.; York, P.; Rowe, R.C.; Roberts, R.J. Effect of Particle Size and Source on Variability of Young's Modulus of MCC Powders. J. Pharm. Pharmacol. **1988**, *40* (suppl), 68 pp.
19. Bassam, F.; York, P.; Rowe, R.C.; Roberts, R.J. Young's Modulus of Powders Used as Pharmaceutical Excipients. Int. J. Pharm. **1990**, *64*, 55–60.
20. Raatikainen, P.; Pöntinen, T.; Ilkka, J.; Ketolainen, J.; Paronen, P. Critical Evaluation of Three Point Bending Test for Measuring Young's Modulus of Pharmaceutical Powders. In Proceedings of 13th Pharmaceutical Technology Conference, Solid Dosage Research Unit, Liverpool, UK, 1994; Rubinstein, M.H., Ed.; Vol. II, 192–203.
21. Raatikainen, P.; Silvennoinen, R.; Ketolainen, J.; Ketolainen, P.; Paronen, P. Evaluation of Pharmaceutical Beam Bending Tests Using Double-Exposure Holographic Interferometry. Eur. J. Pharm. Biopharm. **1997**, *44*, 261–267.
22. Whistler, R.; Daniel, J. Molecular Structure of Starch. In *Starch. Chemistry and Technology*; Whistler, R.; BeMiller, J.; Paschall, E., Eds.; Academic Press: London, 1984; 153–183.
23. French, D. Organization of Starch Granules. In *Starch. Chemistry and Technology*; Whistler, R.; BeMiller, J.; Paschall, E., Eds.; Academic Press: London, 1984; 184–247.